

Research Article

Open Access



Effect of ausforming on isothermal transformation below the martensite start temperature in NiCrMoV steel: an *in-situ* neutron diffraction study

Wu Gong^{1,2} , Stefanus Harjo¹, Takuro Kawasaki¹, Takayuki Yamashita^{1,3}, Akinobu Shibata^{2,4,5}, Tomoya Shinozaki⁶, Yo Tomota^{5,7}, Nobuhiro Tsuji^{2,4}

¹J-PARC Center, Japan Atomic Energy Agency, Naka-gun 319-1195, Japan.

²Elements Strategy Initiative for Structural Materials, Kyoto University, Kyoto 606-8501, Japan.

³Joining and Welding Research Institute, Osaka University, Ibaraki 567-0047, Japan.

⁴Department of Materials Science and Engineering, Kyoto University, Kyoto 606-8501, Japan.

⁵Research Center for Structure Materials, National Institute for Materials Science, Tsukuba 305-0047, Japan.

⁶Steel Casting and Forging Division, Kobe Steel, Ltd., Takasago 676-8670, Japan.

⁷Graduate School of Science and Engineering, Ibaraki University, Hitachi 316-8511, Japan.

Correspondence to: Dr. Wu Gong, J-PARC Center, Japan Atomic Energy Agency, 2-4 Shirane Shirakata, Tokai-mura, Naka-gun 319-1195, Japan. E-mail: wu.gong@j-parc.jp

How to cite this article: Gong, W.; Harjo, S.; Kawasaki, T.; Yamashita, T.; Shibata, A.; Shinozaki, T.; Tomota, Y.; Tsuji, N. Effect of ausforming on isothermal transformation below the martensite start temperature in NiCrMoV steel: an *in-situ* neutron diffraction study. *Microstructures* **2025**, *5*, 2025087. <https://dx.doi.org/10.20517/microstructures.2025.26>

Received: 26 Feb 2025 **First Decision:** 28 Apr 2025 **Revised:** 9 May 2025 **Accepted:** 19 May 2025 **Published:** 4 Aug 2025

Academic Editors: Nima Haghdadi, Huijun Li **Copy Editor:** Shu-Yuan Duan **Production Editor:** Shu-Yuan Duan

Abstract

In-situ neutron diffraction during the thermomechanical controlled processing was employed to investigate the effect of ausforming on isothermal transformation below the martensite start temperature (M_s) in the NiCrMoV steel. After the occurrence of athermal martensitic transformation during cooling of the austenitized sample, the isothermal transformation below the M_s proceeded in two distinct stages: Stage 1, characterized by a rapid transformation rate, and Stage 2, which progressed more slowly. Ausforming suppressed both the athermal martensitic transformation and isothermal transformation in Stage 1 through mechanical stabilization. In contrast, ausforming accelerated the isothermal transformation in Stage 2, likely due to the enhanced carbon diffusion, indicating bainitic transformation characteristics in this stage. The resulting microstructure consisting of tempered martensite, bainite and retained austenite exhibited an excellent strength-ductility balance, achieving an ultimate tensile strength of 1989 MPa, a uniform elongation of 7.1%, and a total elongation of 16%. The present study provides new insights into phase transformation mechanisms below M_s and demonstrates the potential of ausforming-assisted processing for enhancing the mechanical properties of high-strength steels.



© The Author(s) 2025. **Open Access** This article is licensed under a Creative Commons Attribution 4.0 International License (<https://creativecommons.org/licenses/by/4.0/>), which permits unrestricted use, sharing, adaptation, distribution and reproduction in any medium or format, for any purpose, even commercially, as long as you give appropriate credit to the original author(s) and the source, provide a link to the Creative Commons license, and indicate if changes were made.



Keywords: Ausforming, bainitic transformation, martensitic transformation, *in-situ* neutron diffraction, microstructure, mechanical properties

INTRODUCTION

Microstructures in steels, which can be tailored through thermomechanical controlled processing (TMCP), play a crucial role in determining their mechanical properties. Optimizing the microstructures enhances strength, toughness, and ductility, making steels more suitable for high-performance applications in the automotive, aerospace, and structural industries. Among various microstructures in steels, bainite has attracted great attention due to its exceptional balance of strength and ductility, making it a key component in advanced steels such as transformation-induced plasticity (TRIP) and quenching and partitioning (Q&P) steels. Notably, the lath size of bainite structures decreases with decreasing the formation temperature, significantly enhancing mechanical properties^[1-4]. Additionally, the changes in retained austenite (RA) and carbides, including the volume fraction, stability, and morphology of RA^[2,5], as well as the amount, shape, and distribution of carbides^[6], further influence the mechanical properties. These microstructures result from the competition of bainitic transformation, carbon partitioning, and carbide formation during the TMCP process. Consequently, lowering bainitic transformation temperature, particularly in the development of super bainite (or nano-bainite steel), has attracted considerable interest^[2,4,5]. However, conventional steels typically have low carbon and alloy contents to maintain good weldability. In such cases, reducing the isothermal holding temperature can cause it to fall below the martensite start temperature (M_s) of the steels. Isothermal transformations can still occur below the M_s , and numerous studies have classified these transformations as either isothermal martensitic^[7-13] or bainitic transformation^[14-20]. However, distinguishing between bainite and tempered martensite through microstructure observation alone is difficult^[14,17,21], leading to the ongoing debate regarding the nature of isothermal transformation below M_s . This uncertainty highlights the need for further investigation.

Ausforming (i.e., predeformation of austenite) has been explored as a strategy to enhance the mechanical properties of steels by altering the kinetics of phase transformations and the resulting microstructures^[18,22-26]. In recent years, the hot stamping process has gained significant attention for its ability to produce high-strength automotive components. For example, the tensile strength of 22MnB5 steel has been increased to 1,500 MPa using this method^[27]. Hot stamping involves heating steel blank to the austenite phase, forming it into the desired shape, and rapidly quenching it below the M_s in a closed tool to achieve a multiphase microstructure. This growing interest motivates our investigation into the effect of ausforming on phase transformation below the M_s . Ausforming parameters, such as deformation temperature and strain, strongly affect phase transformations, microstructures, and the resulting mechanical properties. Although extensive research has been conducted on the effects of ausforming on martensitic and bainitic transformations, several unresolved issues remain, probably due to the limitations of *in-situ* characterization techniques. For example, ausforming has been reported to lower the M_s temperature due to mechanical stabilization^[23,24]. In contrast, large-strain ausforming has been reported to suppress the bainitic transformation due to mechanical stabilization^[22], while slight-strain ausforming has been shown to accelerate it^[25].

This study aims to clarify the effects of ausforming on phase transformations during isothermal holding below the M_s temperature, focusing on the kinetics of the phase transformation at various stages. As ausforming refines the microstructure, it complicates the quantitative distinction of individual phases using conventional microstructure observations.

The development of high-resolution and high-power neutron diffractometers with exceptional temporal resolution has enabled *in-situ* neutron diffraction techniques to precisely track bulk-averaged

crystallographic information in a short time, including phase fraction^[25,28-30], phase stress^[30], element partitioning^[29], and dislocation density^[28-30]. Furthermore, the engineering neutron diffractometer 'TAKUMI' at J-PARC, equipped with a thermomechanical processing simulator, provides unique capabilities for *in-situ* neutron diffraction studies under extreme conditions^[29,30].

In this study, *in-situ* neutron diffraction was used to investigate the effects of ausforming on phase transformation behavior during isothermal holding below the M_s in NiCrMoV steel. The kinetics of phase transformations during both cooling and isothermal holding stages were quantitatively analyzed on a macroscopic scale. By combining *in-situ* neutron diffraction with microstructure observations, this research aims to distinguish bainitic and martensitic transformations below the M_s , and clarify the effect of ausforming on these phase transformations.

MATERIALS AND METHODS

The NiCrMoV steel with the chemical composition shown in Table 1 was used in this study. This steel was specifically selected due to its sufficient hardenability, which facilitates the control of the TMCP by avoiding ferrite transformation, even at slow cooling rates^[31]. The steel was prepared using vacuum induction melting. The ingots were hot forged into 20 mm square billets and subsequently homogenized at 1,453 K for 1 h, followed by air cooling to ambient temperature.

Cylindrical specimens with a length of 11 mm and a diameter of 6.6 mm were machined from the billets for *in-situ* neutron diffraction experiments. *In-situ* neutron diffraction during TMCP experiments were conducted using the engineering neutron diffractometer 'TAKUMI' at J-PARC^[32]. A thermomechanical processing simulator (Thermecmastor-Z) with a maximum load capacity of 50 kN installed on the diffractometer was used [Figure 1A]. The geometric arrangement for the *in-situ* tests is shown in Figure 1B. The south and north detector banks, each equipped with 5 mm-wide radial collimators, were positioned at +90° and -90° relative to the incident beam [Figure 1B]. The longitudinal direction (compression direction) of the specimen was perpendicular to both the incident neutron beam and the diffracted neutrons detected by the detector banks. Consequently, the scattering vectors of both detector banks were aligned parallel to the radial directions of the specimen. More details on the *in-situ* neutron diffraction experiments can be found in previous papers^[29,30]. The TMCP-treated specimens were *ex-situ* measured using the configuration shown in Figure 1C. The specimen was set horizontally with its longitudinal axis angled at -45° relative to the incident beam, thereby the scattering vectors of the diffraction patterns measured by the north and south detector banks are parallel to the longitudinal and transverse directions, respectively.

Two processes with and without ausforming were performed, as illustrated in Figure 1D. In the non-ausforming case, the specimens were first austenitized at 900 °C for 5 min, followed by cooling to a temperature region of 300 ~ 200 °C at a rate of 10 °C/s. The specimens were then held isothermally before being cooled to ambient temperature. This process is hereinafter denoted as direct isothermal holding (DIH). The ausforming process followed the same procedure as the non-ausforming case, with the addition of a 30% reduction in height via compressive deformation at a strain rate of 0.1 s⁻¹ at 450 °C before the isothermal holding step. This process is hereinafter denoted as ausforming and isothermal holding (AIH). In our previous work^[25], a low strain ausforming was found to accelerate bainitic transformation compared to high strains. Based on this finding, a relatively low strain was selected for the present study. Ausforming was carried out within the bay between ferritic and bainitic transformations at the lowest possible temperature to minimize recovery^[33]. The detailed parameters for each TMCP process are listed in Table 2.

Table 1. Chemical composition of the studied steel (wt.%)

C	Ni	Cr	Mo	V	Si	Mn	Fe
0.30	3.7	1.6	0.49	0.10	0.09	0.31	Bal.

Table 2. Parameters of TMCP processes

	Cooling rate	Deformation	Holding temperature	Holding time
Continue cooling	1 °C/s	-	-	-
DIH	10 °C/s,	-	300 °C, 250 °C, 230 °C, 200 °C	45 min 90 min
AIH	10 °C/s,	450 °C, 30%, 0.1 s ⁻¹	300 °C 250 °C, 230 °C, 200 °C	45 min 90 min

TMCP: thermomechanical controlled processing; DIH: direct isothermal holding; AIH: ausforming and isothermal holding.

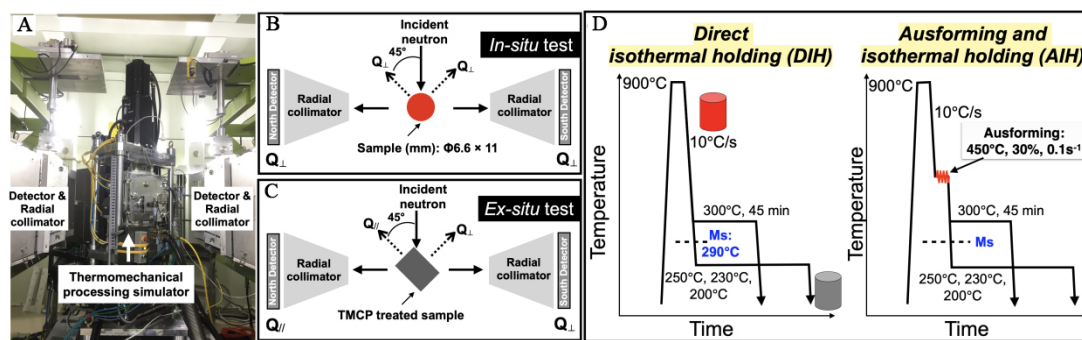


Figure 1. (A) The appearance of the thermomechanical processing simulator on the diffractometer 'TAKUMI'; Diffraction geometries used for (B) *in-situ* and (C) *ex-situ* neutron diffraction experiments; (D) Schematic illustration of the DIH and ausforming and AIH processes, i.e., non-ausforming and ausforming cases, respectively. DIH: Direct isothermal holding; AIH: ausforming and isothermal holding.

Diffraction profiles were analyzed using the Z-Rietveld software to examine changes in lattice parameters and peak intensities^[34]. The volume fraction of each phase was quantified based on the integrated intensities of hkl peaks^[30]. All experimental errors were attributed to the statistical uncertainties of profile fitting.

The microstructures of the specimens were characterized using a JEOL JSM-7800F scanning electron microscope (SEM), while crystallographic orientations were analyzed with a TSL electron backscatter diffraction (EBSD) system mounted on a JEOL JSM-7100F SEM. Specimens were prepared through mechanical grinding followed by etching in a 3% nital solution. For EBSD observations, specimens were electrolytically polished in a solution of 90% CH₃COOH and 10% HClO₄. EBSD data were post-processed using the commercial TSL orientation imaging microscopy (OIM) analysis software.

The mechanical properties of specimens subjected to various TMCPs were evaluated via tensile testing. The cylindrical specimens used for tensile tests were slightly larger than those for *in-situ* neutron diffraction measurements, with dimensions of 12 mm in length and 8 mm in diameter. TMCP experiments were conducted using a Thermecmaster-Z system with a maximum load capacity of 100 kN. Dog-bone-shaped micro-tensile specimens, with a gauge length of 2 mm, width of 1.2 mm, and thickness of 0.6 mm, were extracted from the center of the TMCP-treated specimens. The total length and width of the micro-tensile specimens were 8.0 mm and 3.2 mm, respectively. The tensile and width directions of the plate-type tensile specimens were perpendicular and parallel to the longitudinal axis of the cylindrical specimens, respectively.

Tensile tests were performed using a Shimadzu AG-X Plus system at an initial strain rate of $8.3 \times 10^{-4} \text{ s}^{-1}$ at ambient temperature. The tensile strains of the micro-tensile specimens were precisely measured using the digital image correlation (DIC) method. The details of the specimen dimensions and DIC measurement are shown in [Supplementary Figure 1](#).

RESULTS

Martensitic transformation during continuous cooling

The initial microstructure of the steel was a ferrite matrix with carbides distributed throughout [[Figure 2A](#)]. To determine the M_s and the kinetics of the martensitic transformation, *in-situ* neutron diffraction measurement was conducted on a specimen during continuous cooling from the austenitized condition. As shown in the temperature history in [Figure 2B](#), the specimen was austenitized at 900 °C and subsequently cooled to ambient temperature at a rate of 1 °C/s. The corresponding evolution of neutron diffraction patterns is presented in [Figure 2C](#), plotted on the same horizontal axis scale as [Figure 2B](#). The disappearance of ferrite peaks, along with the appearance and growth of austenite peaks, indicates the occurrence of reverse transformation during reheating to 900 °C. Full austenite was obtained after austenitization at 900 °C [[Figure 2C](#)]. Austenite remained stable during cooling until the temperature decreased to 290 °C. Below 290 °C, martensite peaks appeared, accompanied by a decrease in austenite peak intensity, indicating that M_s was 290 °C. The volume fraction of martensite, as shown in [Figure 2B](#), gradually increased as the temperature decreased further. After cooling to ambient temperature, faint austenite peaks were still observed in the diffraction patterns [[Figure 2D](#)], indicating the presence of RA with a volume fraction of 3.7% [[Figure 2B](#)].

Effect of isothermal holding temperature on kinetics of phase transformation

With the M_s temperature determined, the kinetics of phase transformations in DIH processes with isothermal holding temperatures of 300 °C (above M_s) and 250 °C, 230 °C, and 200 °C (below M_s) were evaluated. [Figure 3](#) presents a comparison of the volume fractions of the body-centered cubic (BCC) phase (including martensite and isothermally transformed product) formed during cooling and isothermal holding at various temperatures. At 300 °C [[Figure 3A](#)], the bainitic transformation began immediately, with the volume fraction of bainitic ferrite gradually increasing and nearing completion after 45 min of holding. After cooling to ambient temperature, only a small fraction of RA (1.2%) was observed.

Below the M_s , the specimens exhibited different features compared to that above the M_s . When the austenitized specimen was cooled to 250 °C, more than half of the austenite (61.1%) transformed into martensite instantaneously through athermal martensitic transformation [[Figure 3B](#)]. During the subsequent isothermal holding at 250 °C, the transformation rate slowed down, with approximately 35.4% of austenite underwent isothermal transformation over 90 min. The amount of RA after cooling to ambient temperature was 2.5%, indicating that about 1 % of austenite transformed to martensite during the final cooling.

As the isothermal holding temperature further decreased, the volume fraction of martensite formed during cooling increased gradually: 61.1% at 250 °C, 71.7% at 230 °C, and 76.0% at 200 °C. In contrast, the volume fraction of isothermally transformed products decreased gradually: 35.4% at 250 °C, 15.9% at 230 °C, and 8.5% at 200 °C. Consequently, the volume fraction of RA increased with decreasing isothermal holding temperature, reaching a maximum of 15.5% at 200 °C.

Characterization of the isothermally transformed products below the M_s

As mentioned earlier, isothermal martensitic transformation and bainitic transformation have been proposed to explain the isothermal transformation occurring below the M_s . To elucidate the characteristics

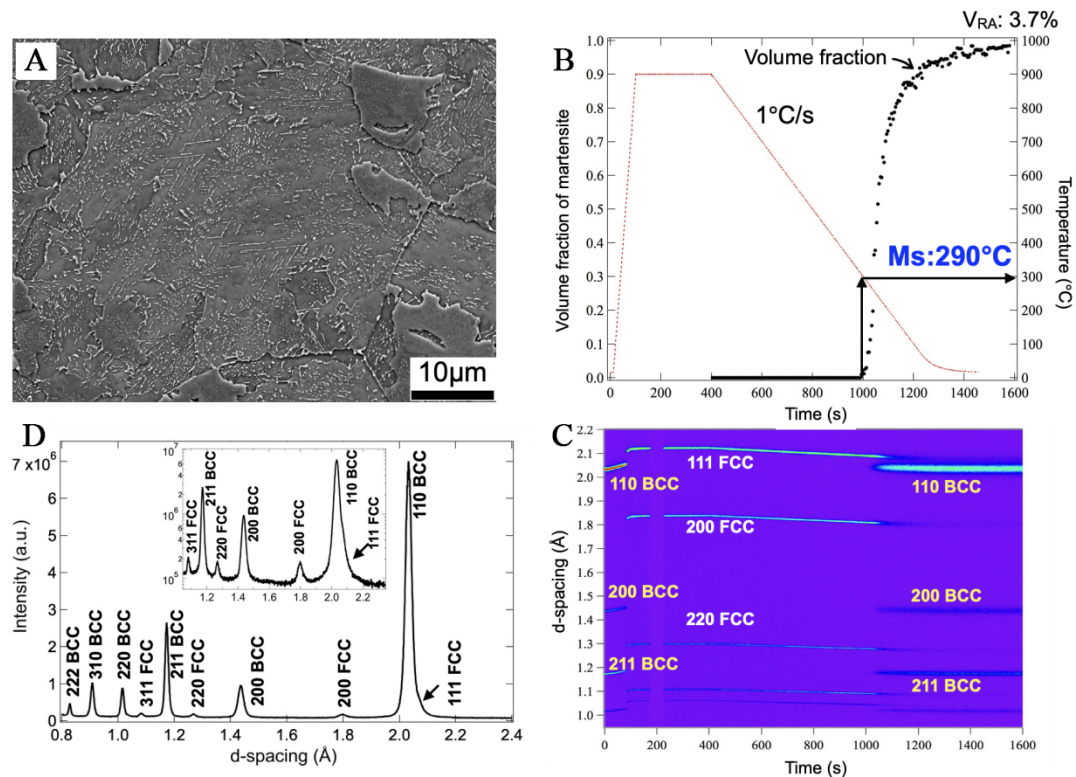


Figure 2. (A) SEM image of the initial microstructure of the NiCrMoV steel; (B) Temperature history and the corresponding changes in volume fraction of martensite; (C) Evolution of diffraction patterns during heat treatment; (D) Diffraction pattern after the heat treatment shown in (B). V_{RA}: Volume fraction of retained austenite at ambient temperature after the process.

of the isothermally transformed products, the microstructures generated by three specific heat treatment processes were compared. The details of these processes are outlined below and schematically represented in [Supplementary Figure 2](#).

- (1) Full bainite: A specimen was subjected to the DIH process with isothermal holding at 320 °C (above Ms) for 90 min.
- (2) Tempered martensite: A specimen was quenched to ambient temperature after full austenitization at 900 °C to obtain martensite with a slight amount of RA, followed by tempering at 230 °C for 90 min.
- (3) Tempered martensite and isothermally transformed products: Two specimens were subjected to the DIH process with isothermal holding at 250 °C and 230 °C (below Ms) for 90 min, respectively.

[Figure 4](#) presents SEM microstructures of the specimens, revealing distinct carbide morphologies between bainite and tempered martensite. In bainite formed at 320 °C [[Figure 4A](#) and [C](#)], carbide platelets were predominantly aligned along a single crystallographic orientation within the bainitic ferrite laths, with additional fine carbides forming at lath boundaries. This distribution aligns with typical lower bainite characteristics reported in prior studies^[35,36] and is illustrated schematically in [Figure 4C'](#). The dense carbide precipitation observed here corresponds to that limited retained austenite presented [[Figure 3A](#)], as the carbon in bainitic ferrite primarily precipitated as carbide, rather than enrichment in austenite.

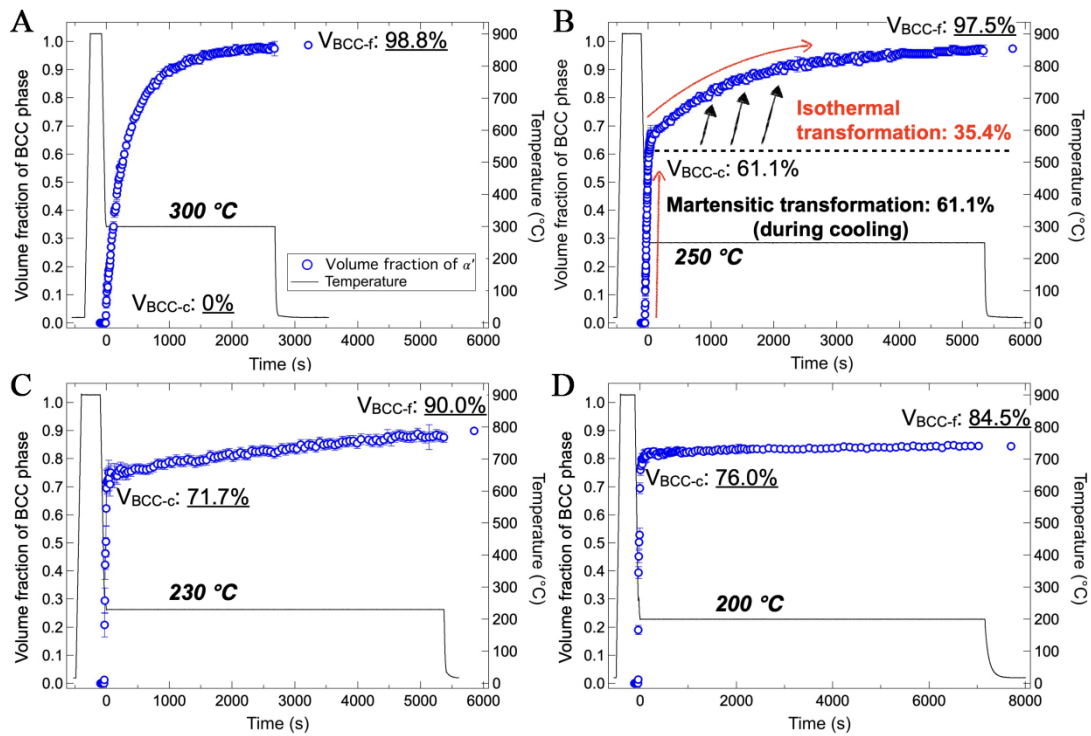


Figure 3. Evolution of the volume fraction of the BCC phase (martensite + bainitic ferrite) in DIH processes with holding temperature of (A) 300 °C (above Ms); and (B) 250 °C; (C) 230 °C; and (D) 200 °C (below Ms). V_{BCC-c} : Volume fraction of BCC formed during cooling; SEM: Scanning electron microscope; V_{BCC-f} : Volume fraction of BCC at ambient temperature after the process. BCC: body-centered cubic; DIH: direct isothermal holding; Ms: martensite start temperature.

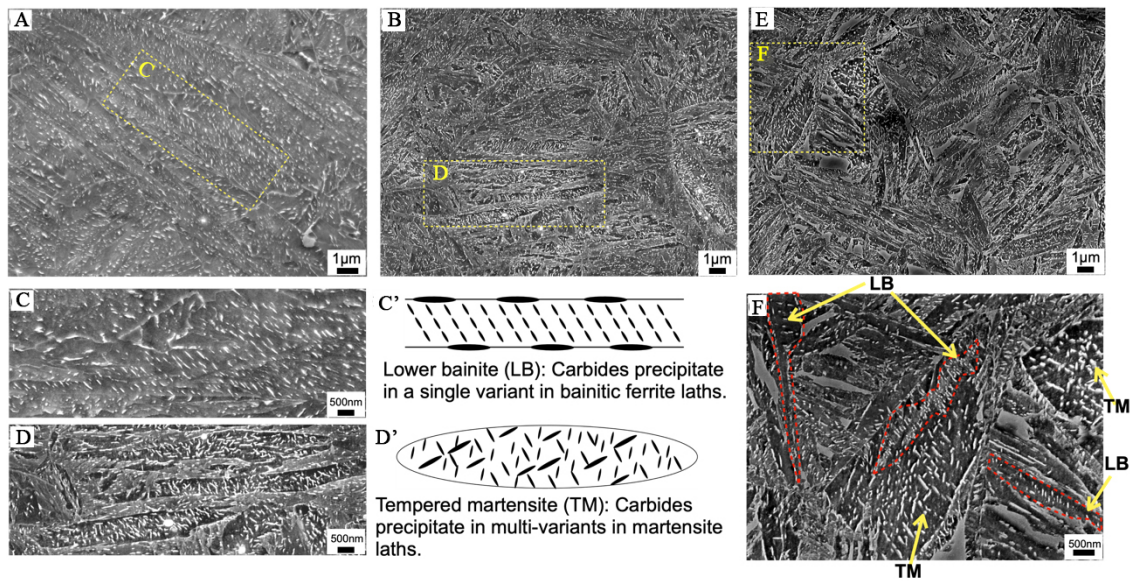


Figure 4. SEM images of specimens subjected to (A) isothermal holding at 320 °C for 90 min and (B) quenching to ambient temperature followed by tempering at 230 °C for 90 min. (C) and (D) Enlarged views of the rectangular areas in (A) and (B), highlighting typical LB and TM, respectively. Schematic illustration of (C') LB and (D') TM. SEM microstructures obtained by (E) isothermal holding at 250 °C for 90 min, and (F) presents the enlarged views of the rectangular areas in (E). SEM: Scanning electron microscope; LB: lower bainite; TM: tempered martensite.

In contrast, tempered martensite exhibited carbides with multiple crystallographic orientations [Figure 4B and D], as represented in Figure 4D'. Such multi-variant carbide precipitation is characteristic of tempered martensite^[13,14,37], where lower transformation temperatures provide sufficient chemical driving force for the simultaneous growth of carbide variants^[37]. By comparison, bainitic transformation suppresses this multi-variant behavior. Carbon partitioning into untransformed austenite during the growth of bainitic ferrite reduces the chemical driving force for carbide precipitation, leading to single-variant carbide precipitation within the bainitic ferrite laths^[38].

In the specimen isothermally held at 250 °C [Figure 4E], the carbides exhibited two distinct characteristics: large tempered martensite (TM) laths with multi-variant carbides (marked as TM in Figure 4F) and ferrite laths containing single-variant carbides. The latter microstructure is similar to lower bainite (LB) (marked as LB in the red areas of Figure 4F).

Further lowering the isothermal holding temperature to 230 °C resulted in the microstructure shown in Figure 5A. Numerous tempered martensite plates can be observed (e.g., the yellow area in Figure 5B), surrounded by lamellar ferrite laths alternating with RA [Figure 5B and C]. These ferrite laths exhibited minimal carbide precipitation, with the carbide platelets aligned in the same direction (see red arrows in Figure 5B). As temperature decreases, the carbide precipitation slows down, and carbon tends to partition into austenite rather than form carbides^[38]. Carbon partitioning promotes the formation of a lamellar structure composed of bainitic laths and RA, which is frequently observed in lower bainitic steels^[4,25]. EBSD analysis of the same region confirmed that the bainitic ferrites shared the same crystallographic orientation as the surrounding martensite [Figure 5C]. This observation suggests that dislocations formed to accommodate martensitic shear strain preferentially promote bainitic ferrite variants that match the existing martensite crystallographic orientation^[28,39,40]. As a result, the microstructure isothermally transformed at 230 °C consisting of tempered martensite, surrounded by bainitic ferrite of the same variant and RA, are schematically illustrated in Figure 5C'.

In a short summary, when the isothermal holding temperature falls below M_s , athermal martensite forms during cooling, followed by isothermal transformation. The final microstructure includes tempered martensite, bainite, and RA. As holding temperature decreases, carbon preferentially enriches into austenite, increasing its stability^[38,41]. Consequently, a higher volume fraction of RA can be obtained at lower temperatures, consistent with the results presented in the previous section.

Effect of ausforming on the kinetics of phase transformation

As martensitic and bainitic transformations both occurred during DIH below the M_s , understanding the effect of ausforming on the kinetics of these phase transformations is of significant interest. Figure 6 presents a comparison of the volume fractions of the BCC phase (including martensite and isothermally transformed product) between DIH and AIH processes.

At 300 °C, ausforming exhibited minimal effect on the kinetics of bainitic transformation [Figure 6A]. This is different from previous studies, where ausforming was found to either suppress bainitic transformation due to mechanical stabilization^[22], or accelerate it at small ausforming strains^[25]. It is important to note that bainitic transformation in the present steel was accompanied by carbide precipitation, whereas previous studies have reported carbide-free bainitic transformation due to the suppression of carbide precipitation by silicon addition. This suggests that the effect of ausforming may differ depending on the extent of carbon partitioning and carbide precipitation.

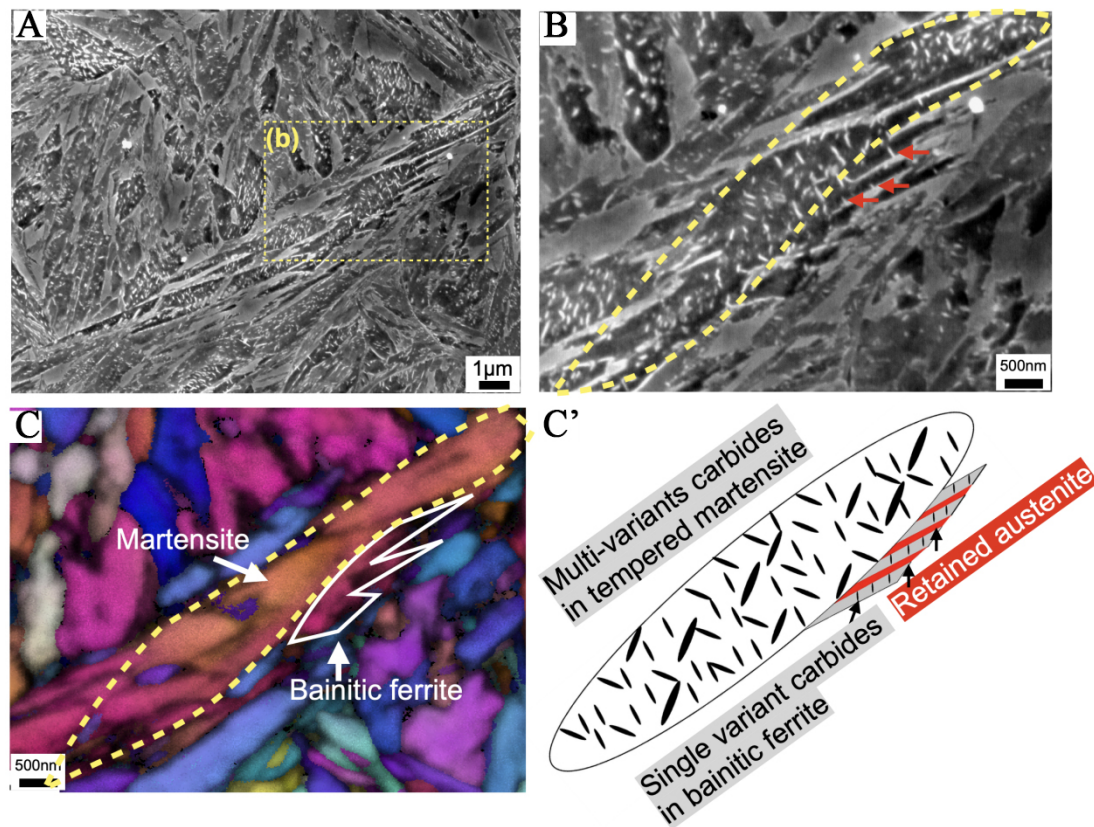


Figure 5. SEM images of specimens subjected to (A) isothermal holding at 230 °C for 90 min; (B) Enlarged SEM image and (c) EBSD IPF map of the rectangular area highlighted in (A); (C') Schematic illustration of the transformed microstructure, consisting of tempered martensite and bainite. SEM: Scanning electron microscope; EBSD: electron backscatter diffraction; IPF: inverse pole figure.

For isothermal holding temperatures below the M_s , ausforming was observed to suppress martensitic transformation that occurred during cooling [Figure 6B–D]. The reductions in volume fraction of martensite due to ausforming were 10.4% at 250 °C, 7.0% at 230 °C, and 4.9% at 200 °C. This suppression can be attributed to mechanical stabilization^[23,24], where ausforming hardens the austenite, making it more difficult to plastically accommodate the shear strain generated during martensitic transformation. However, the volume fractions of the BCC phase formed during isothermal holding at 250 °C and 230 °C in AIH specimens were comparable to those in the DIH specimens [Figure 6B and C]. At 200 °C, the isothermal transformation in the AIH specimen proceeded even faster than in the DIH specimen. The differing effects of ausforming depending on phase transformations at various stages are discussed in Section 4.1. Note that the microstructures of the AIH specimen were refined, making it difficult to distinguish different microstructures as the DIH specimen has done. For reference, SEM images of the AIH specimens have been provided in Supplementary Figure 3.

Figure 7 presents the volume fraction of RA in the final microstructure for both AIH and DIH specimens. In the DIH specimens, the volume fraction of RA increased as the isothermal holding temperature decreased, reaching a maximum value of 15.5% at 200 °C. In contrast, the RA fraction in the AIH specimens was higher than in the DIH specimens at both 250 °C and 230 °C, with a maximum of 16.9% at 230 °C. The RA fractions in the AIH and DIH specimens were comparable at 200 °C. These results suggest that ausforming enhanced the stability of austenite, leading to a higher volume fraction of RA.

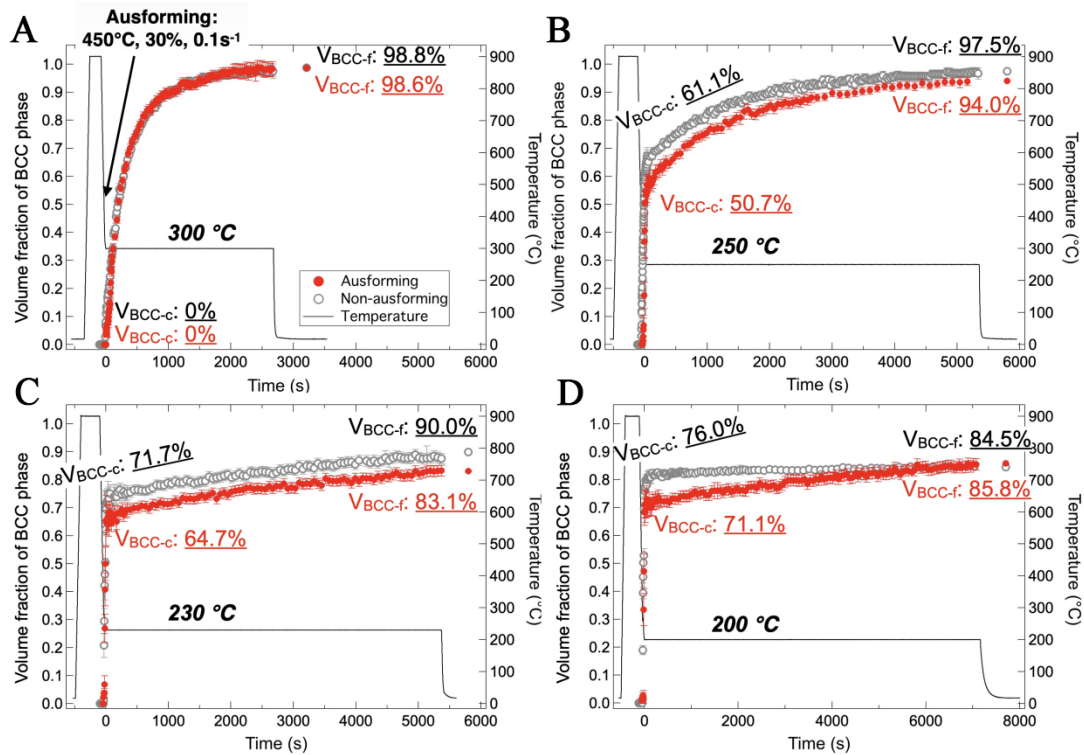


Figure 6. Evolution of the volume fraction of the BCC phase (martensite + bainitic ferrite) in AIH processes with holding temperatures of (A) 300 °C (above Ms); and (B) 250 °C; (C) 230 °C; and (D) 200 °C (below Ms). For comparison, the volume fractions of the BCC phase in DIH processes are included. V_{BCC-c}: Volume fraction of BCC formed during cooling; V_{BCC-f}: Volume fraction of BCC at ambient temperature after the process. BCC: body-centered cubic; AIH: ausforming and isothermal holding; Ms: martensite start temperature; DIH: direct isothermal holding.

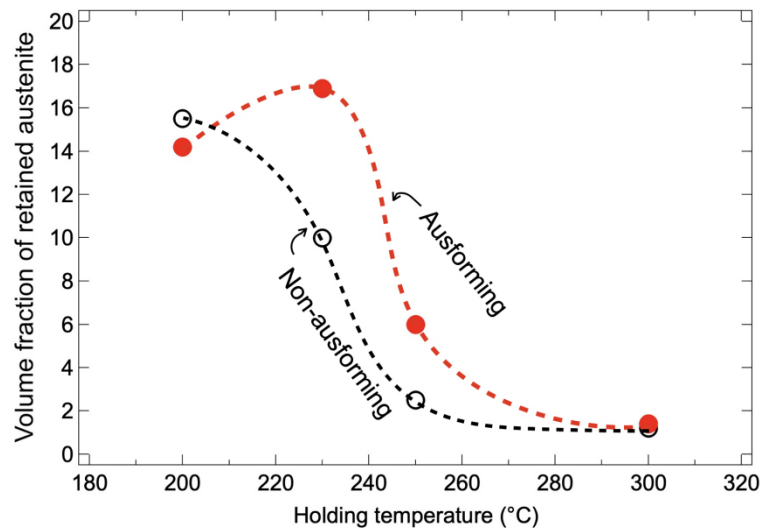


Figure 7. Comparison of volume fraction of retained austenite between AIH and DIH processes in the final microstructure after cooling to ambient temperature. AIH: Ausforming and isothermal holding; DIH: direct isothermal holding.

DISCUSSION

NiCrMoV steel is widely used in various fields as a high-strength material for large forgings. To prevent

heat treatment cracks in large products, quenching (water or oil cooling) is stopped at the temperatures near the M_s , and the product is then transferred to a furnace below the M_s for isothermal treatment. Therefore, it is both academically and industrially significant to understand the effects of ausforming on the phase transformation behavior below the M_s point and its impact on the resulting mechanical properties. The following discussion will focus on two key aspects: the kinetics of isothermal transformation and the mechanical properties.

Effect of ausforming on the kinetics of isothermal transformation below the M_s

The experimental results confirmed the occurrence of isothermal transformation below the M_s in NiCrMoV steel, forming a microstructure consisting of tempered martensite, bainite, and RA. However, there remains uncertainty about whether this isothermal transformation can be fully classified as a bainitic transformation or if it partially involves an isothermal martensitic transformation. The possibility of isothermal martensitic transformation below M_s was first reported by Kurdjumov and Maksimova in 1950^[7]. Since then, extensive research has been carried out on the thermal activation nature of martensitic transformation, particularly in steels with high alloy content and low M_s temperatures^[8-13]. The kinetics of the isothermal martensitic transformation have been reported to be strongly influenced by thermal fluctuations^[42-44] and, consequently, depend on temperature. On the other hand, several studies have reported that bainitic transformation is responsible for the isothermal transformation occurring below the M_s ^[14-20]. The kinetics of bainite formation in this regime are strongly influenced by prior athermal martensite, which provides additional nucleation sites^[19,20]. To quantify the kinetics of isothermal transformation, the transformation rate R_{BCC} was calculated using the equation:

$$R_{BCC} = \frac{\Delta V_{BCC}}{\Delta t}$$

Where ΔV_{BCC} and Δt present the incremental differences in the volume fraction of isothermally transformed products and holding time, respectively.

Figure 8 shows the comparison of the R_{BCC} values between AIH and DIH specimens as a function of the volume fraction of transformed products, V_{BCC} . At 300 °C [Figure 8A], the bainitic transformation of both specimens followed a log-normal distribution, similar to trends observed in other bainitic steels^[19,20]. The kinetics of bainite formation are widely regarded as a displacive transformation mechanism, attributed to the heterogeneous distribution of defects acting as nucleation sites. These defects comprise both pre-existing sites (e.g., austenite grain boundaries) and autocatalytically generated defects arising during transformation^[45,46]. Pre-existing nucleation sites, primarily located at austenite grain boundaries, are gradually consumed as the phase transformation progresses. Conversely, autocatalytically generated defects, which emerge from strain accommodation at the bainite/austenite interface, have been reported to follow a Gaussian distribution^[47]. The AIH specimen exhibited slightly higher transformation rates at a later stage compared to the non-ausformed specimen. This slight increase in transformation rate may be attributed to the enhanced nucleation sites introduced by the lattice defects resulting from ausforming^[25]. Notably, the effect of ausforming on the kinetics of the bainitic transformation at 300 °C was limited, as shown in Figure 6A.

As demonstrated in Figure 8B-D, the isothermal transformation below the M_s in both AHI and DIH specimens exhibited a two-stage evolution, based on the transformation rate R_{BCC} . Stage 1 is characterized by an initially rapid transformation rate followed by a sharp decline, whereas Stage 2 exhibits a slower, progressively diminishing rate. The initial R_{BCC} value in Stage 1 exceeded that of Stage 2 by approximately fivefold. In both stages, R_{BCC} decreased with decreasing temperature, leading to a lower fraction of

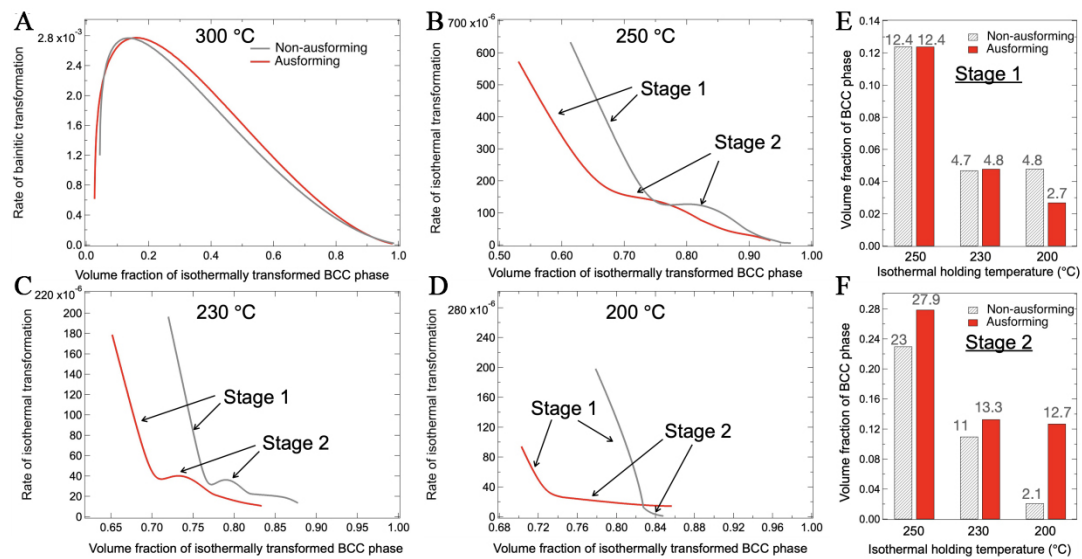


Figure 8. Rate of isothermal transformation in AIH and DIH processes as a function of volume fraction of α' phase at isothermal holding temperatures of (A) 300 °C; (B) 250 °C; (C) 230 °C; and (D) 200 °C. Comparison of the volume fraction of the BCC phase formed during (E) Stage 1 and (F) Stage 2 in AIH and DIH processes, at various isothermal holding temperatures. AIH: Ausforming and isothermal holding; DIH: direct isothermal holding; BCC: body-centered cubic.

isothermally transformed products at lower temperatures. A comparative analysis of R_{BCC} kinetics between AIH and DIH specimens as a function of holding time is provided in [Supplementary Figure 4](#). [Figure 8E](#) and [F](#) compare the increments of volume fraction of BCC phase in the two stages between AIH and DIH specimens, revealing three critical trends:

- (1) The volume fraction of the BCC phase formed during both stages decreased systematically with temperature.
- (2) Ausforming suppressed phase transformation in Stage 1, likely due to strain-induced stabilization of austenite.
- (3) Ausforming enhanced transformation kinetics in Stage 2, particularly at 200 °C.

Hsu *et al.* reported a similar two-stage isothermal transformation in AISI 52100 bearing steel, attributing Stage 1 to the continued growth of athermal martensite and Stage 2 to fresh nucleation and growth of martensite from untransformed austenite^[12]. Kajiwar *et al.* proposed that the rate of isothermal martensitic transformation is governed by the thermally activated motion of lattice dislocations in austenite to accommodate plastically the shear strain of martensite^[10]. As a result, isothermally transformed martensite nucleates from pre-existing martensite and forms the same orientation as the pre-existing one, influenced by prior plastic accommodation in the surrounding austenite^[48]. Similarly, Kim *et al.* found that in low-carbon steel, transformation below M_s occurs through the thickening of pre-existing martensitic laths rather than the formation of new ones, indicating that isothermal transformation below M_s is more characteristic of martensitic rather than bainitic transformation^[13]. Conversely, Ravi *et al.* reported that isothermal transformation below M_s belongs to bainitic transformation, with Stage 1 dominated by rapid bainite formation at prior martensite/austenite interfaces and Stage 2 driven by nucleation at austenite grain boundaries and bainite/austenite interfaces^[19].

The two stages exhibited significantly different transformation rates and opposite sensitivity to ausforming, suggesting distinct transformation mechanisms. Martensitic transformation is typically accompanied by plastic accommodation in the surrounding austenite. The plasticity accommodation hardens the austenite, increasing its mechanical resistance to further transformation. Therefore, an additional driving force, primarily in the form of undercooling, is required to progress the transformation. Additionally, the recovery of dislocations in austenite can relax localized stress and reduce elastic strain energy barriers, allowing the progress of isothermal martensitic transformation^[11]. Due to its displacive nature, ausforming has frequently been reported to suppress martensitic transformation through mechanical stabilization^[23,24]. In contrast, bainitic transformation may progress through the displacive mechanism, meaning mechanical stabilization can also suppress bainitic transformation^[22]. In the meantime, carbon enriches the surrounding austenite. Since carbon diffusion in austenite is significantly slower than in ferrite^[49], this leads to carbon enrichment at the austenite/bainitic ferrite interface^[50]. The carbon enrichment stabilizes the untransformed austenite, slowing further transformation, i.e., the incomplete transformation phenomenon^[51]. Transformation can resume when carbon concentration at the interface decreases due to carbide precipitation or diffusion into austenite grain interior^[52,53]. Consequently, the bainitic transformation rate is primarily controlled by carbide precipitation kinetics and carbon diffusion in austenite. According to the above difference in mechanism, ausforming primarily suppresses martensitic transformation through mechanical stabilization. However, ausforming may exhibit the opposite effect on bainitic transformation: suppressing the transformation due to mechanical stabilization while also accelerating transformation by enhancing carbon diffusion. Note that austenite grain size is a critical factor that affects martensitic transformation kinetics^[54]. However, there is no dynamic recrystallization in the present study due to the low strain and low deformation temperature. The austenite grains exhibited only slight flattening. Therefore, dislocation is considered the dominant factor affecting the subsequent phase transformation.

Figure 6 confirms that ausforming suppressed athermal martensitic transformation, supporting the mechanical stabilization effect. Similarly, ausforming suppressed isothermal transformation in Stage 1, particularly at 200 °C [Figure 8E], suggesting the displacive nature. At 300 °C, ausforming exhibited a minimal effect on bainitic transformation. At this temperature, carbide precipitation dominated [Figure 4A], and the resistance caused by carbon enrichment was negligible, allowing bainitic transformation to proceed rapidly. At lower temperatures, particularly at 200 °C, ausforming accelerated isothermal transformation in Stage 2 [Figure 8F]. Due to the inherently slow diffusion rate of carbon in austenite^[49], localized carbon enrichment at the ferrite/austenite interface hinders further transformation. The acceleration effect of ausforming in Stage 2 is likely attributed to the increased dislocation density in austenite, which enhanced carbon diffusion via pipe diffusion^[55,56]. This reduction in localized carbon concentration at the interface promoted bainitic transformation. This assumption is supported by the difference in carbon enrichment between the AIH and DIH specimens. Figure 9 shows the lattice parameter variations of austenite during holding at 200 °C in AIH and DIH specimens. The lattice parameter in the AIH specimen shows a relatively higher increasing slope than that in the DIH specimen, indicating more carbon enriched in the austenite grain interior in the former, as the solute carbon expands the austenite lattice^[57]. Notably, the initial difference in austenite lattice parameters between the two specimens may be influenced by martensitic transformation^[30] and predeformation, which introduced transformation strain and residual stress, respectively. Therefore, we focused on the slope during isothermal holding rather than the initial gap. Overall, Stage 2 of isothermal transformation exhibited characteristics similar to bainitic transformation, while Stage 1 was less dependent on carbon diffusion and more characteristic of martensitic transformation.

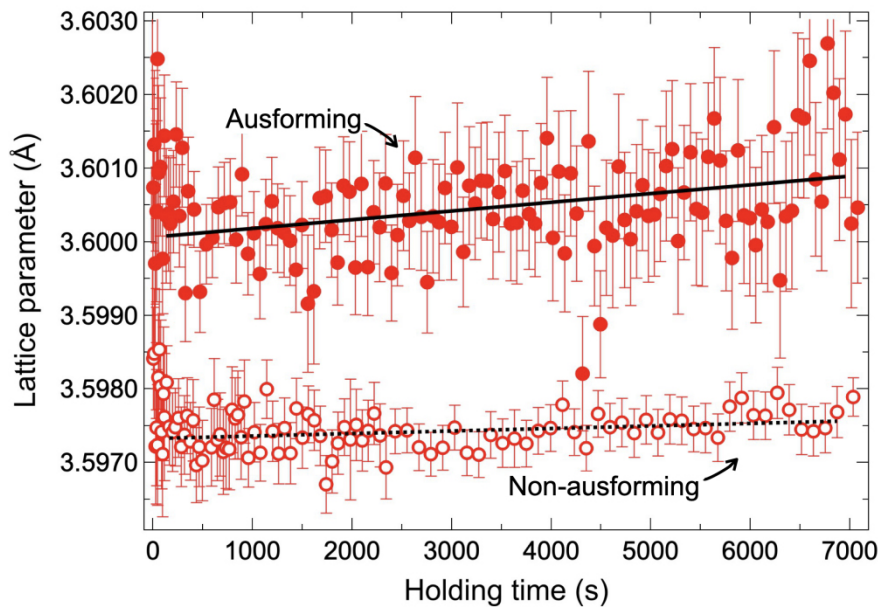


Figure 9. Comparison of lattice parameter changes in austenite during isothermal holding at 200 °C between AIH and DIH processes. The black line and the dotted line represent the linear fits of the lattice parameters in the AIH and DIH processes, respectively. AIH: Ausforming and isothermal holding; DIH: direct isothermal holding.

Effect of ausforming and isothermal holding temperature on mechanical properties

The influence of ausforming on the kinetics of martensitic transformation during cooling and isothermal transformation below the M_s temperature resulted in distinct multiphase microstructures in NiCrMoV steel. To evaluate the mechanical properties of these microstructures, tensile tests were conducted on three representative specimens.

Figure 10 presents the engineering stress-strain curves. The DIH specimen treated at 320 °C consisting of lower bainite and a small fraction of RA [Figure 4A], exhibited a 0.2% proof yield stress (YS) of 1,295 MPa, an ultimate tensile strength (UTS) of 1,521 MPa, and a uniform elongation (UE) of 4.2%. It also showed significant post-necking elongation, resulting in a total elongation of 20%. The DIH specimen treated at 230 °C, containing tempered martensite, bainitic ferrite, and RA [Figure 5A], displayed a higher UTS of 1,756 MPa and a greater UE of 5.9% but a lower YS of 1,130 MPa. The reduction in YS is likely due to the higher volume fraction of RA, which easily transforms into martensite due to its low stability. This needs further investigation to be fully clarified. Compared to the specimen treated at 320 °C, the increase in strength can be attributed to the harder phases, such as tempered martensite and deformation-induced martensite.

A further enhancement in mechanical properties was observed in the AIH specimen treated at 230 °C. This specimen achieved a YS of 1,217 MPa and a UTS of 1,989 MPa while maintaining a UE of 7.1%. The inverse pole figure (IPF) images of the BCC phase in AIH and DIH specimens treated at 230 °C are compared in insets of Figure 10. The average lath size, i.e., the average equivalent area grain size, was determined using OIM software based on the EBSD data. The AIH specimen exhibited a more refined microstructure, with an average lath size of 2.1 μm , smaller than the 3.3 μm in the DIH specimen. Additionally, ausforming increased the RA content [Figure 7], which likely contributed to improved strength and uniform elongation through deformation-induced martensitic transformation. Overall, these results indicate that both ausforming and a reduction in isothermal holding temperature enhanced the strength and ductility of NiCrMoV steel simultaneously.

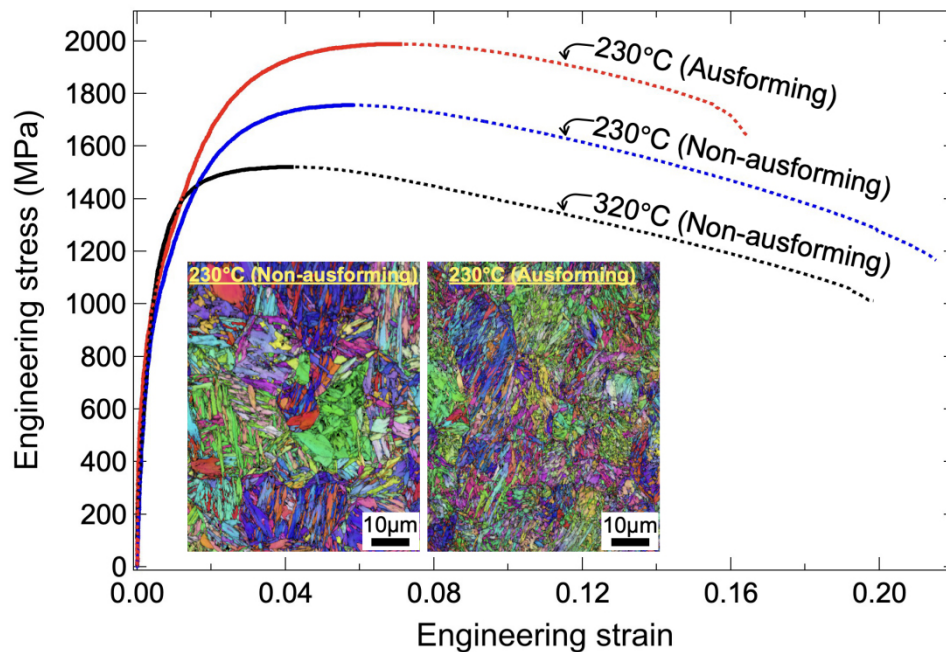


Figure 10. Comparison of engineering stress-strain curves for specimens subjected to AIH and DIH processes at different isothermal holding temperatures. The insets show a comparison of IPF images of the BCC phase in specimens subjected to the AIH and DIH processes treated at 230 °C. IPF: Inverse pole figure; BCC: body-centered cubic; AIH: ausforming and isothermal holding; DIH: direct isothermal holding.

CONCLUSIONS

This study examined the effect of ausforming on isothermal transformation below the M_s in NiCrMoV steel using *in-situ* neutron diffraction. By quantitatively analyzing phase transformation kinetics at different stages, we elucidated the effects of ausforming and isothermal holding temperature on microstructure evolution and mechanical properties. The key findings are as follows:

- (1) After the athermal martensitic transformation during cooling, isothermal transformation occurred in two distinct stages below the M_s : a rapid initial transformation (Stage 1) followed by a slower transformation (Stage 2).
- (2) Ausforming suppressed the athermal martensitic transformation during cooling and isothermal transformation in Stage 1. In contrast, ausforming accelerated the isothermal transformation in Stage 2 by enhancing carbon diffusion in austenite, suggesting the bainitic transformation characteristic.
- (3) Isothermal thermal holding below the M_s produced a multiphase microstructure consisting of tempered martensite, carbide-containing bainite, and retained austenite.
- (4) The volume fraction of retained austenite increased with decreasing isothermal holding temperature and was further increased by ausforming.
- (5) The combination of a lower isothermal holding temperature and ausforming enhanced both strength and ductility in NiCrMoV steel, offering a promising strategy for improving mechanical performance through microstructure control.

DECLARATIONS

Acknowledgments

The neutron diffraction experiments at the Materials and Life Science Experimental Facility of the J-PARC were performed under a general program (Project Nos. 2016A0136, 2016B0252, and 2018L0400).

Authors' contributions

Conception and design of the study: Gong, W.; Tsuji, N.

Investigation: Gong, W.; Harjo, S.; Tomota Y.; Tsuji, N.

Writing: Gong, W.

Methodology: Gong, W.; Harjo, S.; Kawasaki, T.; Yamashita, T.; Shibata, A.

Material preparation: Shinozaki, T.

Supervision and funding acquisition: Tsuji, N.

All authors have reviewed and edited the manuscript and agreed to the submission.

Availability of data and materials

The data that support the findings of this study are available from the corresponding author upon reasonable request.

Financial support and sponsorship

This work was primarily supported by the Elements Strategy Initiative for Structural Materials (ESISM) at Kyoto University. W. G. acknowledges financial support from JSPS KAKENHI (Grant No. JP23K04429).

Conflicts of interest

Shinozaki T. is affiliated with Kobe Steel Ltd. The other authors declared that there are no conflicts of interest.

Ethical approval and consent to participate

Not applicable.

Consent for publication

Not applicable.

Copyright

© The Author(s) 2025.

REFERENCES

1. Ohmori, Y.; Ohtani, H.; Kunitake, T. The mechanical properties of low-carbon low-alloy bainitic steels. *ISIJ. Int.* **1972**, *12*, 146-54. DOI
2. Garcia-mateo, C.; Caballero, F. G. Ultra-high-strength bainitic steels. *ISIJ. Int.* **2005**, *45*, 1736-40. DOI
3. Singh, S.; Bhadeshia, H. Estimation of bainite plate-thickness in low-alloy steels. *Mater. Sci. Eng.: A.* **1998**, *245*, 72-9. DOI
4. Caballero, F. G.; Bhadeshia, H. K. D. H.; Mawella, K. J. A.; Jones, D. G.; Brown, P. Very strong low temperature bainite. *Mater. Sci. Technol.* **2002**, *18*, 279-84. DOI
5. García-mateo, C.; Caballero, F. G. The role of retained austenite on tensile properties of steels with bainitic microstructures. *Mater. Trans.* **2005**, *46*, 1839-46. DOI
6. Ohtani, H.; Okaguchi, S.; Fujishiro, Y.; Ohmori, Y. Morphology and properties of low-carbon bainite. *Metall. Trans. A.* **1990**, *21*, 877-88. DOI
7. Kurdjumov, G. V.; Maksimova, O. P. Kinetics of the transformation of austenite into martensite at low temperatures. *Dokl. Akad. Nauk.* **1948**, *61*, 83-6. Available from: <https://chemport-n.cas.org/chemport-n/?APP=ftslink&action=reflink&origin=npg&version=1.0&coi=1%3ACAS%3A528%3ADyaH1MXksFc%3D&md5=028fa2d6d383701e12ceaf69833079f2> (accessed on 2025-8-1)
8. Thadhani, N. N.; Meyers, M. A. Kinetics of isothermal martensitic transformation. *Prog. Mater. Sci.* **1986**, *30*, 1-37. DOI
9. Pati, S.; Cohen, M. Nucleation of the isothermal martensitic transformation. *Acta. Metallurgica.* **1969**, *17*, 189-99. DOI

10. Kajiwar, S. Mechanism of isothermal martensitic transformation. *Mater. Trans., JIM*. **1992**, *33*, 1027-34. DOI
11. Lobodyuk, V. A.; Estrin, E. I. Isothermal martensitic transformations. *Phys. -Usp.* **2005**, *48*, 713-32. DOI
12. Hsu, T. Y.; Yexin, C.; Weiye, C. Isothermal martensite formation in an AISI 52100 ball bearing steel. *Metall. Trans. A*. **1987**, *18*, 1389-94. DOI
13. Kim, D.; Lee, S. J.; De, C. B. C. Microstructure of low C steel isothermally transformed in the M_s to M_f temperature range. *Metall. Mater. Trans. A*. **2012**, *43*, 4967-83. DOI
14. Okamoto, H.; Oka, M. Lower bainite with midrib in hypereutectoid steels. *Metall. Trans. A*. **1986**, *17*, 1113-20. DOI
15. Bohemen, S. M. C.; Santofimia, M. J.; Sietsma, J. Experimental evidence for bainite formation below M_s in Fe-0.66 C. *Scripta. Mater.* **2008**, *58*, 488-91. DOI
16. Samanta, S.; Biswas, P.; Giri, S.; Singh, S. B.; Kundu, S. Formation of bainite below the M_s temperature: kinetics and crystallography. *Acta. Mater.* **2016**, *105*, 390-403. DOI
17. Navarro-López, A.; Hidalgo, J.; Sietsma, J.; Santofimia, M. J. Characterization of bainitic/martensitic structures formed in isothermal treatments below the M_s temperature. *Mater. Charact.* **2017**, *128*, 248-56. DOI
18. Zhao, L.; Qian, L.; Zhou, Q.; et al. The combining effects of ausforming and below- M_s or above- M_s austempering on the transformation kinetics, microstructure and mechanical properties of low-carbon bainitic steel. *Mater. Des.* **2019**, *183*, 108123. DOI
19. Ravi, A. M.; Navarro-López, A.; Sietsma, J.; Santofimia, M. J. Influence of martensite/austenite interfaces on bainite formation in low-alloy steels below M_s . *Acta. Mater.* **2020**, *188*, 394-405. DOI
20. Navarro-lópez, A.; Hidalgo, J.; Sietsma, J.; Santofimia, M. J. Unravelling the mechanical behaviour of advanced multiphase steels isothermally obtained below M_s . *Mater. Des.* **2020**, *188*, 108484. DOI
21. De-castro, D.; Rementeria, R.; Vivas, J.; et al. Examining the multi-scale complexity and the crystallographic hierarchy of isothermally treated bainitic and martensitic structures. *Mater. Charact.* **2020**, *160*, 110127. DOI
22. Shirzadi, A. A.; Abreu, H.; Pocock, L.; Klobčuar, D.; Withers, P. J.; Bhadeshia, H. K. D. H. Bainite orientation in plastically deformed austenite. *Int. J. Mater. Res.* **2009**, *100*, 40-5. DOI
23. Tsuzaki, K.; Fukasaku, S.; Tomota, Y.; Maki, T. Effect of prior deformation of austenite on the $\gamma \rightarrow \epsilon$; martensitic transformation in Fe-Mn alloys. *Mater. Trans., JIM*. **1991**, *32*, 222-8. DOI
24. Maalekian, M.; Kozeschnik, E.; Chatterjee, S.; Bhadeshia, H. K. D. H. Mechanical stabilisation of eutectoid steel. *Mater. Sci. Technol.* **2007**, *23*, 610-2. DOI
25. Gong, W.; Tomota, Y.; Adachi, Y.; Paradowska, A. M.; Kelleher, J. F.; Zhang, S. Y. Effects of ausforming temperature on bainite transformation, microstructure and variant selection in nanobainite steel. *Acta. Mater.* **2013**, *61*, 4142-54. DOI
26. Miyamoto, G.; Iwata, N.; Takayama, N.; Furuhashi, T. Quantitative analysis of variant selection in ausformed lath martensite. *Acta. Mater.* **2012**, *60*, 1139-48. DOI
27. Uenishi, A. Development of advanced high strength sheet steel for NSafTM-AutoConcept. *Nippon. Steel. Sumitomo. Met. Tech. Rep.* **2019**, *118*, 1-6. Available from: <https://www.nipponsteel.com/en/tech/report/pdf/122> (accessed on 2025-8-1)
28. Gong, W.; Tomota, Y.; Harjo, S.; Su, Y. H.; Aizawa, K. Effect of prior martensite on bainite transformation in nanobainite steel. *Acta. Mater.* **2015**, *85*, 243-9. DOI
29. Shibata, A.; Takeda, Y.; Park, N.; et al. Nature of dynamic ferrite transformation revealed by *in-situ* neutron diffraction analysis during thermomechanical processing. *Scripta. Mater.* **2019**, *165*, 44-9. DOI
30. Gong, W.; Harjo, S.; Tomota, Y.; et al. Lattice parameters of austenite and martensite during transformation for Fe-18Ni alloy investigated through *in-situ* neutron diffraction. *Acta. Mater.* **2023**, *250*, 118860. DOI
31. McNaughton, W. P.; Richman, R. H.; Jaffee, R. I. "Superclean" 3.5 NiCrMoV turbine rotor steel: a status report - Part I: steelmaking practice, heat treatment, and metallurgical properties. *J. Mater. Eng.* **1991**, *13*, 9-18. DOI
32. Harjo, S.; Ito, T.; Aizawa, K.; et al. Current status of engineering materials diffractometer at J-PARC. *Mater. Sci. Forum.* **2011**, *681*, 443-8. DOI
33. I. Deformation-induced martensitic transformation and transformation-induced plasticity in steels. *Met. Sci.* **1982**, *16*, 245-53. DOI
34. Oishi-Tomiyasu, R.; Yonemura, M.; Morishima, T.; et al. Application of matrix decomposition algorithms for singular matrices to the Pawley method in Z-Rietveld. *J. Appl. Crystallogr.* **2012**, *45*, 299-308. DOI
35. Bhadeshia, H. K. D. H. The lower bainite transformation and the significance of carbide precipitation. *Acta. Metall.* **1982**, *28*, 1103-14. DOI
36. Ohmori, Y.; Jung, Y. C.; Ueno, H.; Nakai, K.; Ohtsubo, H. Crystallographic analysis of upper bainite in Fe-9% Ni-C alloys. *Mater. Trans., JIM*. **1996**, *37*, 1665-71. DOI
37. Chang, L. C.; Bhadeshia, H. K. D. H. Stress-affected transformation to lower bainite. *J. Mater. Sci.* **1996**, *31*, 2145-8. DOI
38. Bhadeshia, H. K. D. H. *Bainite in Steels*; Institute of Materials: London, 1992.
39. Kawata, H.; Hayashi, K.; Sugiura, N.; Yoshinaga, N.; Takahashi, M. Effect of martensite in initial structure on bainite transformation. *Mater. Sci. Forum.* **2010**, *638-42*, 3307-12. DOI
40. Toji, Y.; Matsuda, H.; Raabe, D. Effect of Si on the acceleration of bainite transformation by pre-existing martensite. *Acta. Mater.* **2016**, *116*, 250-62. DOI
41. Ribamar, G. G.; Escobar, J. D.; Da, S. A. K.; et al. Austenite carbon enrichment and decomposition during quenching and tempering of high silicon high carbon bearing steel. *Acta. Mater.* **2023**, *247*, 118742. DOI

42. Kulin, S. A.; Speich, C. R. J. Isothermal martensite formation in an iron-chromium-nickel alloy. *Metals* **1952**, *4*, 258-63. [DOI](#)
43. Cohen, M.; Machlin, E. S.; Paranjpe, V. G. In *Thermodynamics in Physical Metallurgy*; American Society for Metals: Cleveland, 1950; p 242.
44. Roitburd, A. L.; Kurdjumov, G. V. The nature of martensitic transformations. *Mater. Sci. Eng.* **1979**, *39*, 141-67. [DOI](#)
45. Cohen, M. Martensitic nucleation-revisited. *Mater. Trans., JIM.* **1992**, *33*, 178-83. [DOI](#)
46. Ravi, A. M.; Sietsma, J.; Santofimia, M. J. Exploring bainite formation kinetics distinguishing grain-boundary and autocatalytic nucleation in high and low-Si steels. *Acta. Mater.* **2016**, *105*, 155-64. [DOI](#)
47. Lin, M.; Olson, G. B.; Cohen, M. Distributed-activation kinetics of phase transformations in steel. *Metall. Trans. A.* **1992**, *23*, 2987-98. [DOI](#)
48. S. Continuous observation of isothermal martensite formation in Fe-Ni-Mn alloys. *Acta. Metall.* **1984**, *32*, 407-13. [DOI](#)
49. Santofimia, M. J.; Zhao, L.; Petrov, R.; Sietsma, J.; Van Der Zwaag, S. Influence of interface mobility on the evolution of austenite-martensite grain assemblies during annealing. *Acta. Mater.* **2009**, *57*, 4548-57. [DOI](#)
50. Dai, Z.; Ding, R.; Yang, Z.; Zhang, C.; Chen, H. Elucidating the effect of Mn partitioning on interface migration and carbon partitioning during quenching and partitioning of the Fe-C-Mn-Si steels: modeling and experiments. *Acta. Mater.* **2018**, *144*, 666-78. [DOI](#)
51. Aaronson, H. I.; Reynolds, W. T.; Purdy, G. R. The incomplete transformation phenomenon in steel. *Metall. Mater. Trans. A.* **2006**, *37*, 1731-45. [DOI](#)
52. Kaufman, L.; Cohen, M. Thermodynamics and kinetics of martensitic transformations. *Prog. Met. Phys.* **1958**, *7*, 165-246. [DOI](#)
53. Toji, Y.; Miyamoto, G.; Raabe, D. Carbon partitioning during quenching and partitioning heat treatment accompanied by carbide precipitation. *Acta. Mater.* **2015**, *86*, 137-47. [DOI](#)
54. Celada-Casero, C.; Sietsma, J.; Santofimia, M. J. The role of the austenite grain size in the martensitic transformation in low carbon steels. *Mater. Des.* **2019**, *167*, 107625. [DOI](#)
55. Mimkes, J. Calculations of dislocation pipe diffusion. *J. Phys. Colloques.* **1979**, *C6*, 181-3. [DOI](#)
56. Zorgani, M.; Garcia-Mateo, C.; Jahazi, M. Microstructural evolution during tempering of an ausformed carbide-free low temperature bainitic steel. *Mater. Des.* **2021**, *210*, 110082. [DOI](#)
57. Bhadeshia, H. K. D. H.; David, S. A.; Vitek, J. M.; Reed, R. W. Stress induced transformation to bainite in Fe-Cr-Mo-C pressure vessel steel. *Mater. Sci. Technol.* **1991**, *7*, 686-98. [DOI](#)